Check for updates

RESEARCH ARTICLE

XRD analyses on silica-amended Class G cement samples exposed to clean and impure CO_2 in the presence of water.

[version 1; peer review: 1 approved]

Reinier van Noort

Department of Reservoir Technology, IFE Institute for Energy Technology, Kjeller, Norway

v1 **First published:** 13 Feb 2026, **6**:47
https://doi.org/10.12688/openreseurope.22922.1
Latest published: 13 Feb 2026, **6**:47
https://doi.org/10.12688/openreseurope.22922.1

Abstract

Background and methods

This paper presents XRD analyses on samples of silica-amended Class G Portland Cement exposed to CO_2-saturated water and wet supercritical CO_2, using clean CO_2, CO_2 with 1.6 mol% H_2S, and CO_2 in equilibrium with concentrated H_2SO_4, under conditions relevant for the geological storage of CO_2. The results complement microstructural and chemical analyses on the same samples published previously, for an enhanced insight into the mineralogical changes induced in these samples by exposure, focusing on the impacts of exposure environment (CO_2-saturated water vs. wet supercritical CO_2) and key impurities (H_2S and H_2SO_4) on cement alteration and carbonate formation, as well as on the fate of introduced impurities within the altered cement matrix.

Results

The results show that initial Ca-carbonate precipitation was dominated by metastable vaterite, which subsequently dissolved again and re-precipitated, partly, as more stable calcite and aragonite. During exposure to CO_2-saturated water, vaterite dissolution also resulted in the leaching of significant Ca^{2+} into the aqueous exposure fluid, especially in the presence of H_2S, while during exposure to wet supercritical CO_2 (with or without H_2S), overall carbonate contents continued to increase. During the exposure to CO_2 with H_2SO_4, samples were affected to the presence of H_2SO_4 and desiccation effects, leading, in particular, to relatively high aragonite contents. Exposure in the presence of both H_2S and H_2SO_4 resulted in the formation of, mostly minor quantities of, pyrite and pyrrhotites. In

Open Peer Review

Approval Status ✓

	1
version 1 13 Feb 2026	✓ view

1. **Alastair Marsh**, Ecole Polytechnique Federale de Lausanne Laboratory, Lausanne, Switzerland
Sudharsan Rathna Kumar, Ecole Polytechnique Federale de Lausanne, Lausanne, Switzerland

Any reports and responses or comments on the article can be found at the end of the article.

addition, exposure to CO_2 with H_2S resulted in the precipitation of significant quantities of gypsum, most likely as a result of the oxidation of sulphide to sulphate through the reduction of Fe^{3+} from brownmillerite.

Conclusions

Even though, overall, the impacts of impurities were relatively minor, these results reiterate the need for a thorough, experiment-based understanding of potential impurity-mineral interactions for accurate long-term forecasting of cement integrity during CCS.

Keywords
CCS; Geological CO2 storage; Wellbore integrity; Wellbore sealant; Cement; Sealant; Integrity; Storage integrity



This article is included in the Horizon Europe gateway.

Corresponding author: Reinier van Noort (reinier@ife.no)

Author roles: van Noort R: Conceptualization, Data Curation, Formal Analysis, Investigation, Methodology, Resources, Visualization, Writing – Original Draft Preparation

Competing interests: No competing interests were disclosed.

Grant information: This project has received funding from the European Union's Horizon Europe research and innovation programme under grant agreement No [101094664] (A European Network of Research Infrastructures for CO2 Transport and Injection [ENCASE]). Views and opinions expressed are however those of the author(s) only and do not necessarily reflect those of the European Union. Neither the European Union nor the granting authority can be held responsible for them
The funders had no role in study design, data collection and analysis, decision to publish, or preparation of the manuscript.

Copyright: © 2026 van Noort R. This is an open access article distributed under the terms of the Creative Commons Attribution License, which permits unrestricted use, distribution, and reproduction in any medium, provided the original work is properly cited.

How to cite this article: van Noort R. **XRD analyses on silica-amended Class G cement samples exposed to clean and impure CO_2 in the presence of water. [version 1; peer review: 1 approved]** Open Research Europe 2026, **6**:47 https://doi.org/10.12688/openreseurope.22922.1

First published: 13 Feb 2026, **6**:47 https://doi.org/10.12688/openreseurope.22922.1

Introduction

Portland Cement (PC) is still the main component in sealant materials used as annular seals as well as plugs in subsurface wells. However, PC-based materials are highly reactive with CO_2, especially at the elevated temperatures and pressures expected in reservoirs at several km's depth. This reactivity may lead to challenges to the (long term) integrity of wells exposed to CO_2 during geological carbon storage (GCS – as part of Carbon Capture and Storage; CCS).

As part of the Cementegrity project, Van Noort *et al.*[1,2] exposed samples of five different sealant compositions for up to 16 weeks to clean CO_2, CO_2 with H_2S and CO_2 with H_2SO_4, in the presence of water. During these exposures, sample cylinders were placed both above and below water, to expose them to either wet supercritical CO_2, or CO_2-saturated water. After the experiments, samples were studied and analysed using Scanning Electron Microscopy (SEM) with Energy Dispersive Spectroscopy (EDS), as well as Computed Tomography scanning (CT-scanning). While these analyses showed that exposure to CO_2 with H_2S or H_2SO_4 lead to differences in the microstructure and chemical composition of the reacted zones of exposed samples, mineralogical compositions, and exposure- and impurity-dependent changes in mineralogy were not addressed in these works.

In our previous work[2], we noted that XRD analyses should be performed in order to enhance our understanding of the mineralogical changes induced in the exposed cement samples. Therefore, in this paper I present XRD analyses with Rietveld refinement on an unexposed sample of the sealant denoted as S1 (Class G PC with 35% by weight of cement silica flour), as well as on samples of this sealant exposed to clean CO_2, CO_2 with H_2S, or CO_2 with H_2SO_4, in the presence of water. In particular, I will focus on how the presence of S-based impurities affected the mineral assemblages that formed during CO_2-exposure, and on the fate of these S-based impurities in CO_2 when interacting with PC-based sealants in the GCS reservoir.

Sample preparation and analysis

The cement samples analysed here were batch-exposed to either CO_2-saturated water or wet supercritical CO_2, using clean CO_2, CO_2 containing 1.6 mol% H_2S, or CO_2 in equilibrium with concentrated H_2SO_4. Sealant samples were exposed for up to 16 weeks, with some samples placed near the bottom of the vessel (exposed to CO_2-saturated water) and some samples placed in the top half of the vessel (exposed to wet supercritical CO_2). For a full description of how these samples were prepared and cured, and then exposed, see 1,2. Additional exposures with a duration of 7 days were carried out by placing a single cylinder in a small titanium pot that was in turn placed inside a 100 ml Hastelloy pressure vessel, with either sufficient demineralised water in the titanium pot to fully cover the sample (exposure to CO_2-saturated water), or with water added outside the titanium pot to saturate the CO_2-phase (exposure to wet supercritical CO_2 (see also 3). All samples were cylinders with a length of 30 mm and a diameter of ~12 mm. Note that only samples exposed for 16 weeks were analysed here, as other samples were not available.

Unexposed cylinders were crushed whole to obtain reference samples. For exposed cylinders, samples were prepared for analysis from different parts of the cylinder (see Figure 1), representing the inner, carbonated but intact zone, and different parts of the outer altered zone. For this purpose, first a disc of 2–3 mm was cut off the end of the exposed cylinder using a thin, water-cooled diamond saw. On most samples, top and bottom ends of the cylinders were both available, and easily distinguished. For these samples, discs were cut from both ends, marked as such, and analysed separately. After cutting the sample discs, they were ground down to a thickness of 1.8–2.1 mm on a diamond disc. On the samples exposed for 16 weeks to CO_2-saturated water (with and without H_2S), a thick precipitate layer was deposited on top of the samples. These deposits were scraped off and collected for separate analysis before cutting the top disc off the sample. Note that one end the sample exposed to supercritical CO_2 without impurities (suspected to be the top of the cylinder, though this could not be ascertained with full certainty) looked quite different from the rest of the sample and the other sample exposed simultaneously, in particular as it was much more reddish in colour.

To obtain samples representative of the inner part of the sample, a cylinder of roughly 8 mm was cut closer to the centre of the sample, taking care to avoid visibly altered material from the top and bottom ends of the cylinder. Subsequently, ~3 mm was ground off from the sides of this cylinder, to obtain a roughly octagonal inner core prism with a maximum diameter of ~6 mm.

Finally, to assure a more direct comparison with the radial cross-sections imaged and analysed previously using SEM with EDS (see 1–3), thin vertical slices (1.5–2.0 mm) were cut around the outer rim of the sample, parallel to the cylinder axis. For the samples exposed for 16 weeks to CO_2-saturated water with and without H_2S (where an outer, altered rim was clearly visible) and for the samples exposed for 7 days (where a carbonated rim was clearly visible), extra care was taken to ensure only materials from the outer reaction rim were collected. Note that outer rim samples could not be taken from the sample exposed to supercritical CO_2 with H_2SO_4, as insufficient material was available.

All samples obtained in these manners were gently crushed by hand using an agate mortar and pestle to obtain a fine powder. Before analyses, samples were spiked with Al_2O_3 (Alfa Aesar Aluminum oxide, alpha-phase, 99.99% (metals basis)) as an internal standard for quantification, by mixing 90 mg sample with 10 mg Al_2O_3, to give a spike content of 10±0.5%. Note that this was not done for analysis of the precipitates scraped off the exposed sample cylinders. Furthermore, for some samples additional measurements were performed without Al_2O_3 spike, to ensure that the samples did not contain Al_2O_3 before the spiking. To carry out the analyses, prepared samples were deposited onto a flat silicon plate by wetting the sample holder with isopropanol, and then gently distributing the powdered sample into that. As the isopropanol evaporated, this resulted in a thin, distributed powder layer on the Si-plate. Samples were then

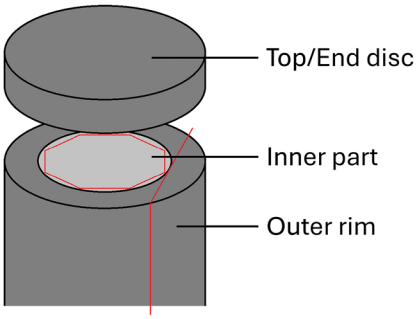


Figure 1. Schematic drawing illustrating the different sample parts cut and prepared for XRD analysis.

analysed in a Bruker D2 phaser, using Cu-radiation and Lynx-Eye XE detector in Bragg-Brentano geometry. The patterns were measured over a 2θ range of 5–70° with a step size of 0.02°, and a count time of 1 s per step.

After analysis, peak identification was performed manually, using Bruker EVA software. Next, Rietveld refinement quantifications for the identified phases, as well as the amorphous content, were performed using the TOPAS V5 software[4]. In the refinement, a 5th order Chebychev background correction was used. In addition, a sample height correction was refined. Two additional (broad) peaks were allowed to improve background fitting. For individual phases, refinements were performed for lattice parameters, crystallite sizes (Lorentzian) and scale factors.

Results

Unexposed reference sample

Table 1 presents quantifications for the XRD analyses performed on all different parts of all exposed samples, as well as an unexposed reference sample. Table 2 provides an overview of all mineral phases included in the quantifications. All data files have all been deposited in an open repository[5]. For the unexposed reference sample, an amorphous content of about 63% is supplemented with ~19% tobermorite-11 Å, ~10% katoite, ~5% brownmillerite (i.e., ferrite), and ~2–3% quartz, mostly matching microstructural observations of a homogeneous cement gel matrix containing some larger quartz particles (see 1). Significant portlandite ($Ca(OH)_2$ – free lime) was not detected, indicating that most Ca^{2+} was bound to the CSH-gel phases. Note that in this quantification, to obtain a strong match between pattern and refinement, eighth order spherical harmonics were used to correct for preferential orientation of the tobermorite.

Exposure to clean CO_2

Different exposure conditions resulted in different chemical and mineralogical compositions, especially in the outer parts of the exposed samples. Short-term (7 days) exposure to CO_2-saturated water resulted in an outer zone, about 3.6 mm wide, where any free $Ca(OH)_2$ had carbonated, and the pH had been reduced below 8.3 (as indicated using phenolphthalein – see 3). Further inwards of this, the material appeared mostly unaffected, and testing with phenolphthalein showed that a high pH (>8.3) was maintained, though minor Ca-leaching or partial carbonation could not be fully excluded. The XRD analyses carried out here (see Figure 2) indeed show the disappearance of tobermorite and katoite from the outer zone, and the precipitation of ~38% carbonates, of which 29% vaterite. In the inner part, tobermorite and katoite are still present (though tobermorite is somewhat reduced). Here, the analysis also shows ~14% carbonates (7% vaterite). However, while care was taken to separate inner and outer parts (based on colour differences), it is possible that some of the carbonated outer material was included in this analysis.

In the sample exposed to wet supercritical CO_2 for 7 days, the carbonated outer zone was ~4.1 mm wide[3]. Here, XRD again shows the removal of tobermorite and katoite, along with the precipitation of 39% carbonates (29% vaterite). In the inner part, tobermorite and katoite contents are again somewhat reduced, and ~27% carbonate was detected (13% vaterite). However, due to small available sample size, here some inclusion of the carbonated outer material cannot be excluded, and this could explain the elevated carbonate content.

As reported previously[1,2], exposure to CO_2-saturated water resulted in significant Ca-leaching from, and alteration and degradation in, the outer part of the exposed sample, while the inner part was strongly carbonated but not altered significantly in its elemental composition. This is reflected in the XRD analyses on the inner and outer parts of the exposed cylinder (see Figure 3). In the inner part of the sample, tobermorite and katoite were no longer found and only minor brownmillerite remained, while carbonation also resulted in the precipitation of 34% carbonates, dominated by vaterite (27%). The nett amorphous content decreased somewhat (to 60%). In the outer part of the sample, 16 week exposure to CO_2-saturated water resulted in the disappearance of nearly all crystalline gel phases (tobermorite and katoite, while some brownmillerite remained), while the carbonate content had decreased to ~25% with calcite (12%) being the prevalent carbonate, along with aragonite and some vaterite). As a result of these changes, the amorphous content had increased to 67%. Analysis of the precipitates scraped off the sample top surface indicated that these consisted mostly of aragonite, with some calcite.

As the relatively high carbonate content measured in the top disc of the exposed sample appeared somewhat contrary to the strongly leached outer zone with highly depleted Ca/Si-ratio reported in Van Noort *et al.*[2], the XRD-analyses were repeated on a bottom disc of the same sample cylinder, as well as on thin (<2 mm thick) slices cut parallel to the cylinder axis, from the altered outer rim. The goal of these additional analyses was to assess how representative the top disc analyses presented here (where Ca-leaching and carbonisation may have been inhibited by the thick precipitate layer) were in comparison to radial cross-sections. In the bottom disc, the overall carbonate content (~27%) was somewhat higher than that measured in the top disc, but, more notably, vaterite (15%) was the main carbonate

Table 1. Rietveld quantifications for exposed cement samples as well as the unexposed reference sample. Fe-(hydr)oxides combines quantifications for goethite and hematite. Fe-sulphides sums pyrite and pyrrhotites. The symbol "-" indicates minerals that were not included in the Rietveld analysis. "ND" indicates minerals that were included in the quantification, but were not detected (<0.05%). *) For the sample exposed to clean wet supercritical CO_2, sample top and bottom were not marked. Disc 2 most likely represents the top, and Disc 1 the bottom.

Exposed to	Impurity	Dur. (d)	Analysed part	Quartz	Tobermorite	Katoite	Brownmillerite	Portlandite	Calcite	Aragonite	Vaterite	Dolomite	Siderite	Fe-(hydr)oxides	Fe-sulphides	Gypsum	Anhydrite	Amorphous
-	-	-	-	2.7	18.9	10.2	5.3	ND	-	-	-	-	-	-	-	-	-	62.8
wet sc. CO_2	-	7	Inner part	4.6	11.7	9.0	4.7	-	12.0	1.3	13.4	-	-	<1	-	-	-	42.5
wet sc. CO_2	-	7	Outer rim	4.5	<1	-	4.6	-	7.9	2.2	29.4	-	-	<1	-	-	-	51.0
CO_2 sat. H_2O	-	7	Inner part	3.0	13.5	7.3	4.1	-	6.4	0.8	7.2	-	-	1.5	-	-	-	56.1
CO_2 sat. H_2O	-	7	Outer rim	3.2	<1	-	4.6	-	5.9	3.2	28.5	<1	-	<1	-	-	-	53.6
wet sc. CO_2	-	112	Inner part	2.9	ND	-	2.3	-	7.8	1.0	27.0	-	-	<1	-	-	-	58.9
wet sc. CO_2	-	112	Disc 2*	11.9	<1	-	1.0	-	13.5	2.1	0.2	-	-	2.5	-	-	-	68.6
wet sc. CO_2	-	112	Disc 1*	3.3	<1	-	1.2	-	6.9	5.9	14.8	-	-	1.0	-	-	-	66.8
wet sc. CO_2	-	112	Outer rim	3.0	<1	-	2.6	-	8.7	8.7	22.3	-	-	<1	-	-	-	53.9
CO_2 sat. H_2O	-	112	Inner part	3.2	ND	-	2.3	-	5.5	1.0	27.4	-	-	<1	-	-	-	59.6
CO_2 sat. H_2O	-	112	Top disc	4.3	ND	-	3.2	-	11.7	8.4	3.8	1.1	-	<1	-	-	-	66.8
CO_2 sat. H_2O	-	112	Bottom disc	5.7	ND	-	1.9	-	7.6	4.3	15.4	ND	-	<1	-	-	-	64.7
CO_2 sat. H_2O	-	112	Outer rim	6.9	ND	-	2.6	-	13.6	7.1	1.5	-	-	1.1	-	-	-	67.2
wet sc. CO_2	H_2S	112	Inner part	4.6	ND	-	2.3	-	7.1	1.3	26.1	-	-	<1	<1	<1	-	57.6
wet sc. CO_2	H_2S	112	Top disc	8.1	ND	-	<1	-	11.0	3.7	8.2	-	<1	<1	1.0	5.2	-	61.3
wet sc. CO_2	H_2S	112	Bottom disc	5.7	ND	-	<1	-	10.5	4.7	17.7	-	<1	<1	<1	1.5	-	57.7
wet sc. CO_2	H_2S	112	Outer rim	3.6	ND	-	2.5	-	10.8	1.8	33.6	-	<1	<1	<1	<1	-	45.6
CO_2 sat. H_2O	H_2S	112	Inner part	3.4	ND	-	2.8	-	7.4	2.1	34.6	-	-	<1	<1	<1	-	48.5
CO_2 sat. H_2O	H_2S	112	Top disc	2.7	ND	-	1.6	-	14.8	7.9	7.2	-	-	<1	<1	<1	-	64.4
CO_2 sat. H_2O	H_2S	112	Bottom disc	4.8	ND	-	2.6	-	9.4	6.6	13.5	-	-	<1	<1	<1	-	61.2
CO_2 sat. H_2O	H_2S	112	Outer rim	10.6	<1	-	<1	-	15.3	3.1	0.0	-	1.1	1.4	1.8	2.4	-	63.9
wet sc. CO_2	H_2SO_4	112	Inner part	3.1	ND	-	4.1	-	11.8	17.5	11.7	-	-	<1	<1	<1	ND	51.3
wet sc. CO_2	H_2SO_4	112	End disc	4.8	<1	-	4.3	-	10.6	11.4	23.3	-	-	<1	<1	ND	<1	44.2
wet sc. CO_2	H_2SO_4	112	Outer rim	6.6	ND	-	4.2	-	11.4	11.3	19.1	-	<1	ND	<1	<1	-	46.6

Open Research Europe 2026, 6:47 Last updated: 22 JUN 2026

Table 2. All minerals with chemical formulas and PDF-identifiers considered in the discussed XRD analyses and quantifications.
Abbreviations as used in Figure 2–Figure 5.

Mineral name	Abbreviation	Chemical formula	PDF-identifier
Anhydrite	-	$CaSO_4$	01-080-6360
Aragonite	A	$CaCO_3$	01-076-0606
Brownmillerite	B	$Ca_2Al_{1.078}Fe_{0.922}O_5$	04-014-6640
Calcite	C	$CaCO_3$	01-078-4614
Corundum	*	Al_2O_3	04-015-8996
Dolomite	-	$CaMg(CO_3)_2$	04-015-9838
Goethite	-	FeO(OH)	04-014-5919
Greigite	-	Fe_3S_4	04-008-7806
Gypsum	G	$CaSO_4.2H_2O$	00-033-0311
Hematite	-	Fe_2O_e	00-033-0664
Katoite	K	$Ca_{2.916}Al_2(SiO_4)_{1.092}(OH)_{7.632}$	01-0754213
Magnetite	-	$Fe_{2.897}O_4$	01-086-1343
Portlandite	-	$Ca(OH)_2$	00-044-1481
Pyrite	-	$FeS_{1.92}$	01-071-5207
Pyrrhotite	P	Fe_7O_8	01-076-2308
Pyrrhotite	-	Fe_9S_{10}	04-025-3489
Pyrrhotite	-	$Fe_{11}S_{12}$	04-017-9146
Quartz	Q	SiO_2	04-027-5352
Siderite	S	$FeCO_3$	04-022-6948
Tobermorite-11Å	T	$Ca_{2.25}Si_3O_{6.5}(OH)_{3.5}$	04-011-0271
Vaterite	V	$CaCO_3$	04-017-8634
Wüstite	-	$Fe_{0.914}O$	04-026-3177

phase here. The amorphous content (65%) was comparable to that measured in the top disc. In the outer rim, the overall carbonate content was somewhat lower (~22%) and dominated by calcite (14%) with aragonite (7%) leaving only little vaterite (~1–2%). The amorphous content (67%) was again comparable to that measured in the top and bottom discs.

In principle, direct exposure to wet supercritical CO_2, as opposed to exposure to a volume of CO_2-saturated water, should not result in significant Ca-leaching and degradation. Indeed, SEM imaging with EDS mapping[1] show that elemental compositions did not change significantly. XRD analyses on the inner part of the sample show that this exposure did lead to the disappearance of crystalline gel phases (with the exception of some brownmillerite) and a carbonate content of ~36%, dominated by vaterite (~27%) and calcite (8%). As a result of these reactions, the nett amorphous content decreased somewhat, similar to the sample exposed to CO_2-satured water (to ~59%). In the first end disc cut off this sample, which was most likely cut from the bottom part, the crystalline gel phases were similarly depleted, while the carbonate content was reduced to ~28%, comprising mostly vaterite (15%) with calcite (7%) and aragonite (6%), leading to an increased amorphous content of 67%. In the second disc (presumed cut from the top), considerably greater changes in mineral composition are observed, with an increase in quartz content to 12% and amorphous content (to 69%), a decrease in overall Ca-carbonate content to 16% (with nearly-complete removal of vaterite) and the appearance of ~2–3% Fe-(hydr)oxides, corresponding well to the dark reddish colouration of this part of the sample. To the contrary, in the outer rim sample, the overall carbonate content had increased to 40%, with a reduced vaterite content (22%) and

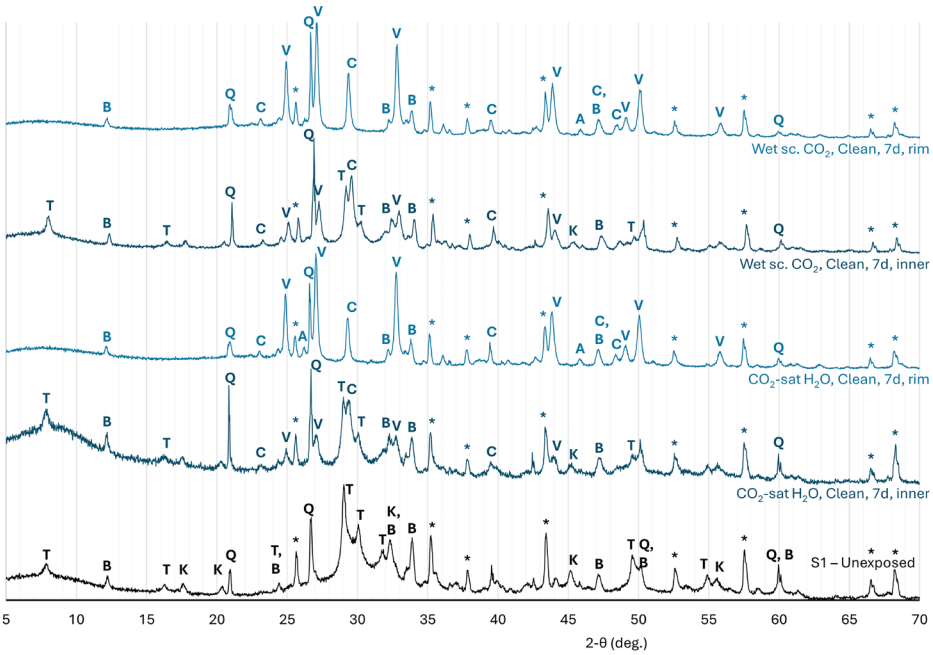


Figure 2. Normalised diffraction patterns measured on an unexposed reference sample of cement S1 (Class G PC with 35% BWOC silica flour), and on samples of the same cement exposed to clean CO_2 for 7 days.

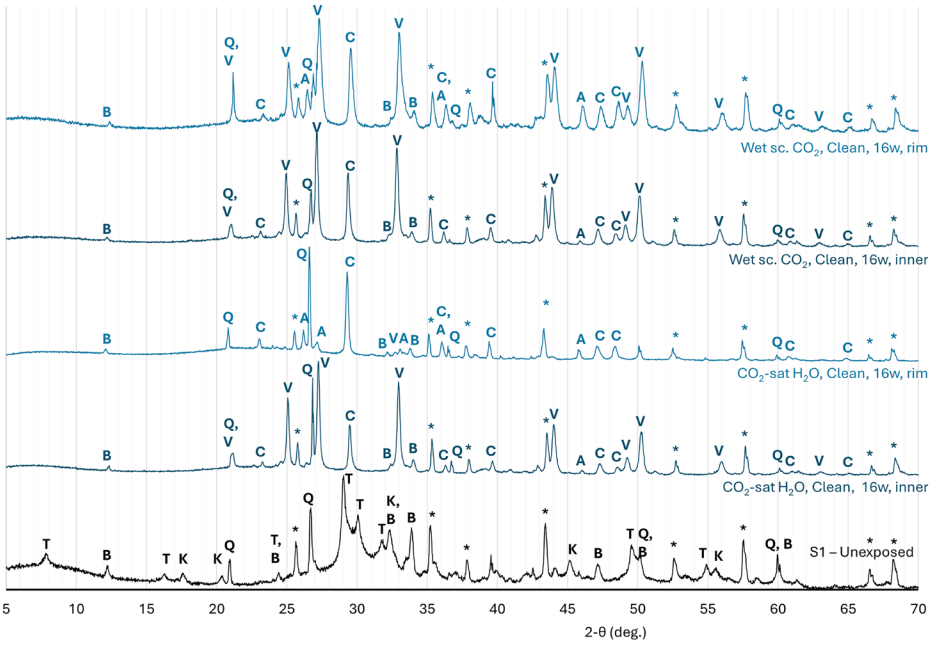


Figure 3. Normalised diffraction patterns measured on an unexposed reference sample of cement S1 (Class G PC with 35% BWOC silica flour), and on samples of the same cement exposed to clean CO_2 for 16 weeks.

increased calcite and aragonite contents (both ~9%). Here, the brownmillerite content was comparable to that measured in the inner part, while the amorphous content had decreased to 54%.

Exposure to CO_2 with H_2S

XRD analyses of the sealant samples exposed to CO_2-saturated water in equilibrium with a CO_2-phase containing 1.6 mol% H_2S

(leading to a H_2S content in the hydrous phase of 0.087 mol% at initial equilibrium – see Figure 4) showed that this exposure again resulted in the disappearance of most of the crystalline gel phases, with the exception of some brownmillerite. However, in the inner part of the sample, a very high carbonate content (44%) was observed, with vaterite being the main carbonate phase (~35%). Furthermore, minor Fe-sulphides (pyrite and pyrrhotites) and gypsum were detected. The amorphous content was about 48%.

In the top disc analysed here, a relatively high carbonate content of ~30% was detected, with calcite as the dominant carbonate phase (15%), along with significant aragonite (8%) and vaterite (7%). The amorphous content had increased to 64%, which can be ascribed mostly due to carbonate removal compared to the inner part of the sample. While a minor increase in S-content was observed in the outer part of exposed samples (when considering the S/Si-ratio – see 2), only minor Fe-sulphides (less than 1% total pyrite and pyrrhotites), as well as minor gypsum were detected by XRD. Analysis of the precipitates scraped off the top of this sample showed that these mainly consisted of aragonite and calcite.

As for the sample exposed to water saturated with clean CO_2, analysis of the sample exposed to water saturated with H_2S-bearing CO_2 was repeated on the bottom disc of the same sample cylinder, as well as on a sample cut from the outer rim. In the bottom disc, a comparable carbonate content of about 29% was observed, though with vaterite (13%) as the dominant carbonate phase. The amorphous content was also comparable, at ~61%. Similarly minor quantities of Fe-sulphides and gypsum were also detected. In the outer rim, however, the overall carbonate content had decreased significantly, to ~19% (dominated by 15% calcite, and including ~1% siderite, while vaterite was not detected). Furthermore, ~2% gypsum and ~2% Fe-sulphides were detected in this part of the sample, while the amorphous content (64%) was comparable to the top disc.

For the sample exposed directly to wet supercritical CO_2 with H_2S, in the inner part of the sample, all crystalline gel phases with the exception of some brownmillerite were removed, while carbonation led to a Ca-carbonate content of 34%, dominated by vaterite (26%) and calcite (7%). With regards to potential S-bearing phases, some Fe-sulphides were again observed here, along with (very) minor gypsum, correlating to a significantly increased S/Si-ratio. In the top part of the sample, the crystalline gel phases were mostly eliminated, while the carbonate content is reduced to about 24%, dominated by calcite (11%) and vaterite (8%). With regards to S-bearing phases, roughly 1% of Fe-sulphides were again observed, but more significantly, exposure in this part of the sample also resulted in the precipitation of ~5% gypsum. In the bottom part of this

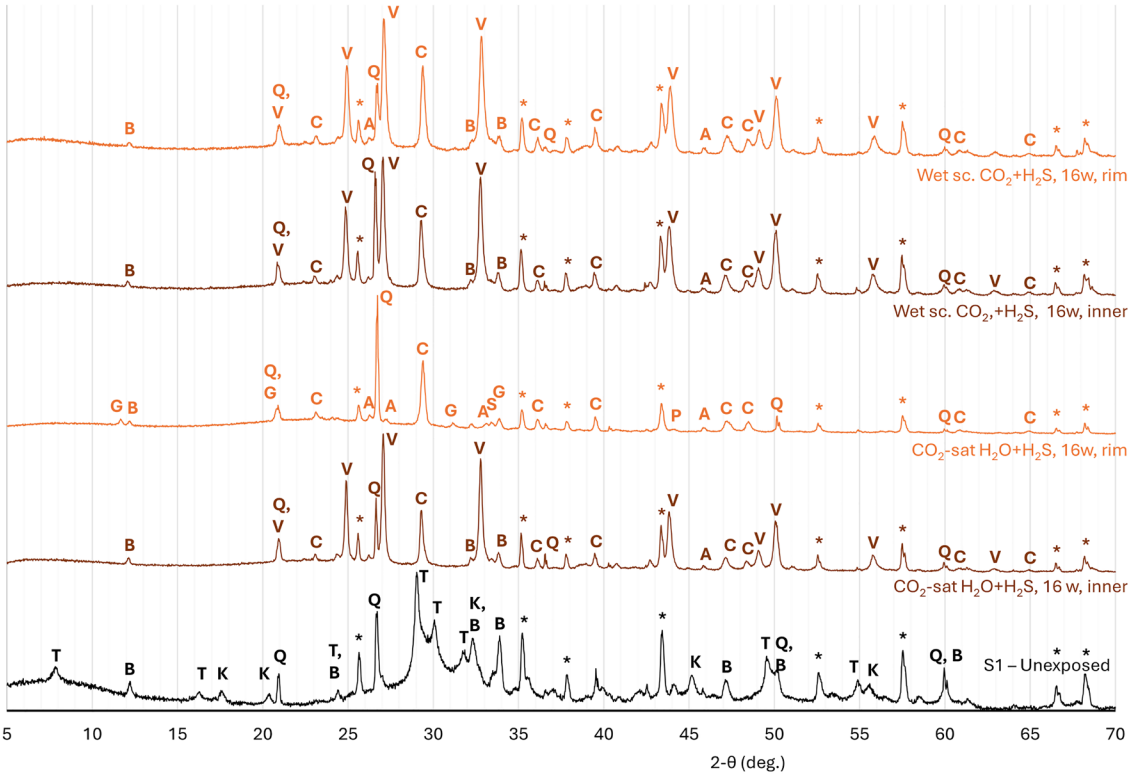


Figure 4. Normalised diffraction patterns measured on an unexposed reference sample of cement S1 (Class G PC with 35% BWOC silica flour), and on samples of the same cement exposed to CO_2 with 1.6 mol% H_2S for 16 weeks.

sample, the amorphous content (58%) and overall carbonate content (33%) were quite similar to the inner part; however, the vaterite content had decreased (to 18%) in favour of calcite (10%) and aragonite (5%), as well as 1–2% gypsum and minor Fe-sulphides. Most notable, the outer rim sample showed a further increase in Ca-carbonate content compared to the inner part (to 47%), with very high vaterite (33%) and somewhat elevated calcite (11%) contents. Contrary to the top and bottom parts of the sample, the analysis on the outer rim showed only negligible gypsum, while some Fe-sulphides and siderite were detected.

Exposure to CO_2 with H_2SO_4

To expose samples to CO_2 containing a realistically low concentration, but significant quantity of SO_3 within the limitations of a batch apparatus, 2 exposed their samples directly to supercritical CO_2 only, while open vials of concentrated H_2SO_4 were placed inside their reaction vessel. This allowed for exchange between the CO_2-phase and the H_2SO_4, resulting in exposure of the samples to SO_3-bearing CO_2. SO_3 would then dissolve into the hydrous phase in the cement pore network and hydrolyse to reform H_2SO_4. However, as discussed by 2, this method also resulted in partial desiccation of the cement samples, which may have inhibited reaction progression.

This is reflected in the XRD analyses of both the inner and outer parts of this sample (see Figure 5), which show the preservation of a higher content (~4%) brownmillerite in the exposed sample, as well as the precipitation of ~41% (inner) to ~45% (end disc) carbonate. Interestingly, while aragonite (17%) was the main carbonate in the inner part of the sample (along with ~12% each of calcite and vaterite), in the outer rim part of the sample, vaterite (19%) made up almost half of the 42% total carbonate content (along with 11% each of calcite and aragonite). Analysis of the end disc showed a higher vaterite content (23%), but similar calcite and aragonite contents (11% each). Only minor Fe-sulphides were detected in both the inner and outer parts of this sample. Interestingly, while very minor gypsum was detected in the inner part and outer rim of the sample, in the end disc analysed, this was replaced by anhydrite.

Discussion and implications

Impact of exposure to clean CO_2

The presented results show that exposure to both CO_2-saturated water and wet supercritical CO_2 first caused the disappearance of the crystalline cement gel phases tobermorite and katoite, while brownmillerite reacted more slowly. As these samples did not contain significant portlandite, the dissolution or leaching of Ca^{2+} from the CSH-gel phases then provided Ca^{2+} for the precipitation of Ca-carbonates, while the leached residues of the gel-phases most likely formed an amorphous Si-rich gel phase, though some crystalline quartz may also have precipitated as indicated by increases in quartz-content in some parts of the exposed samples.

As shown by the analyses on the outer parts of the samples exposed for 7 days, as well as the inner parts of samples exposed for 16 weeks, the dissolved Ca^{2+} initially precipitated locally within the samples, with this initial carbonate precipitation being dominated by metastable vaterite. Such initial precipitation of metastable vaterite instead of more stable Ca-carbonates calcite and aragonite is well documented in the literature (cf. 6–12), and may have been promoted in these samples by high supersaturation and/or the relatively high CO_3^{2-}-content and thus lower Ca^{2+}/CO_3^{2-}-ratio due to high CO_2-pressure and high (initial) pore water pH (cf. 6,13). Subsequently, as seen in the outer parts (top, bottom and outer rim) of the samples exposed for 16 weeks to CO_2-saturated water, the precipitated vaterite dissolved again, and then either reprecipitated locally as more stable aragonite and/or calcite, or was

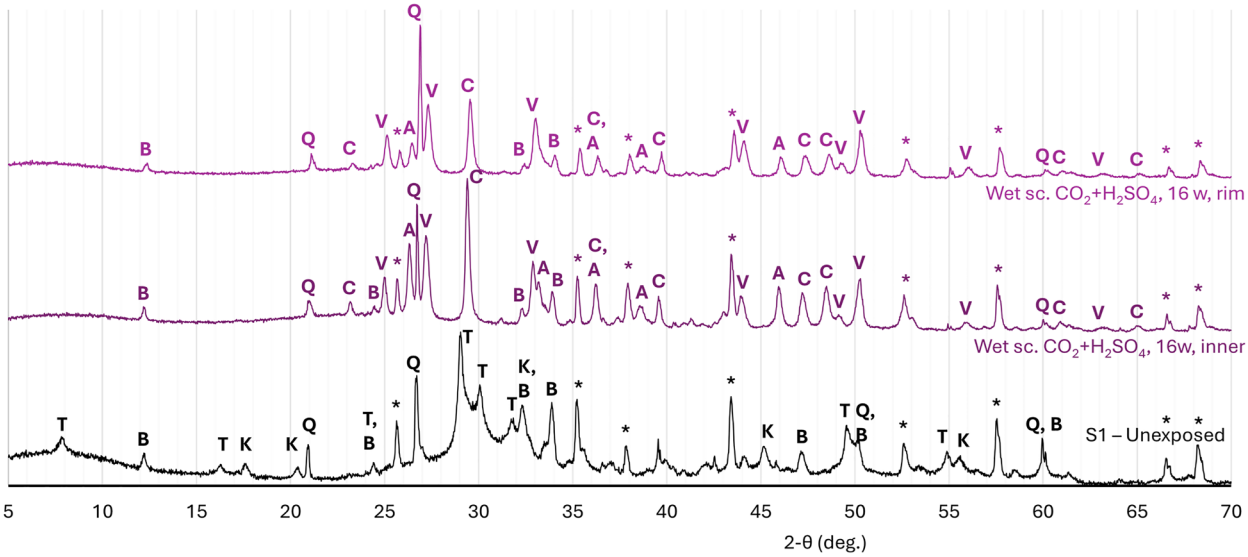


Figure 5. Normalised diffraction patterns measured on an unexposed reference sample of cement S1 (Class G PC with 35% BWOC silica flour), and on samples of the same cement exposed to CO_2 in equilibrium with concentrated H_2SO_4 for 16 weeks.

transported away by diffusion through the pore fluid, leading to a decrease in overall Ca-carbonate content (from 34% to ~25%). Such diffusion was the main mechanism for the observed removal of Ca from, and therefore the degradation of, the exposed samples (see also 1). When comparing the analyses performed on different outer parts of the sample exposed to CO_2-saturated water (top disc, bottom disc, and outer rim), the top disc and outer rim analyses give quite comparable compositions, but the bottom disc shows a higher vaterite content. While the sample holder was constructed with shallow recesses to stably hold the samples, and each recess had a hole to enable fluid access to the bottom surface of the sample (see 1), fluid access to the bottom parts was likely still restricted by the sample holders, inhibiting vaterite dissolution, and limited Ca-leaching from and CO_2-diffusion into the bottom part of the sample. This resulted in slower progression of the alteration reactions here, explaining the relatively high vaterite content and overall Ca-carbonate content. However, it should also be noted that the CT-scanning images presented by 2 showed strong variability in density in the outer part of this sample, ascribed (by them) to different degrees of Ca-leaching and carbonate preservation, and the XRD analyses presented here provide an averaged analysis over the selected volume, and do not differentiate for this variability. Differences in composition between the top disc and the outer rim sample are very limited, suggesting that reactions in the top disc were not impacted significantly by the precipitate layer formed on top of the sample.

Interestingly, in the sample exposed to wet supercritical CO_2, a similar reduction in overall (crystalline) carbonate content was detected between the inner (36%) and outer parts. In the (presumed) bottom part of this sample, both vaterite and calcite contents decreased, while aragonite increased. Here, the reduction in crystalline carbonate content (to 28%) was associated with an equivalent (8%) increase in amorphous content. In the other end disc, the Ca-carbonate content had been reduced very strongly (to ~16%), and was dominated by calcite (13%) while vaterite had disappeared. At the same time, the quartz content in this sample showed a strong increase (to 12%), and significant Fe-(hydr)oxide contents were also measured. However, as noted above, optical observations suggested this top part may have been altered anomalously compared to the rest of the sample as well as the other sample exposed simultaneously. The very strong reduction in carbonate-content (and increase in quartz content) suggest that Ca may have been leached from this sample part, which would require exposure to an aqueous fluid. One mechanism that could have caused this would be water-precipitation driven by a decreasing temperature gradient towards to the top of the exposure vessel leading to a flow of water along the sample. Note that the SEM micrographs presented by 1 do show minor signs of Ca-removal from the outer surfaces of the 4- and 8-week exposed samples, but not the 16-week exposed sample. In this regard, the outer rim sample, showing a strong increase in aragonite, and a minor decrease in vaterite content, as well as an overall increase in carbonate content compared to the inner part of the sample may be the most representative of the impact of exposure to wet supercritical CO_2 without any leaching.

Overall, the samples studied here contained more calcite than aragonite. However, when comparing inner and outer parts of samples exposed for 16 weeks, typically, somewhat greater increases in aragonite than calcite are observed, though in the very strongly altered sample, aragonite had mostly disappeared in favour of calcite. While literature studies on the preferential precipitation of Ca-carbonate polymorphs have shown the preferential formation of aragonite at our exposure temperature (80 °C; cf. 14) pH variations and pore fluid chemistry (e.g., Ca^{2+}/CO_3^{2-}-ratio) may have also affected polymorph selection. Furthermore, in pure $CaCO_3$-H_2O-systems, Ca-carbonate phase transitions from metastable vaterite to calcite or aragonite typically take place within a day[6]. Therefore, the continued existence of vaterite after 16 weeks exposure further supports the notion that in the current samples, Ca-carbonate stability is likely affected by pore fluid chemistry composition factors, such as pH, Ca^{2+}/CO_3^{2-}-ratio, and the presence of (trace amounts of) other compounds, such as metal-cations or sulphate[15], in the system.

Interestingly, the layer of precipitates found on the top surface of the sample exposed to CO_2-saturated water comprised mostly aragonite, with some calcite. Here, the preferential precipitation of aragonite over the other Ca-carbonate polymorphs was likely due to the relatively high Mg/Ca-ratios in the external exposure fluid[16,17], as at the end of the exposure a Mg/Ca molar ratio of 0.9 was measured (see 2). In addition, aragonite precipitation in the exposure fluid outside the sample may also have been promoted by relatively high aqueous carbonate-concentrations (e.g., 16).

Impact of H_2S and H_2SO_4 on the carbonation and degradation processes

Within the carbonated inner parts of the exposed samples, the greatest impact of H_2S was observed in the sample exposed to CO_2-saturated water. Here, the presence of H_2S resulted in a significantly higher vaterite content and overall carbonate content when compared to the equivalent sample exposed to CO_2-saturated water without H_2S. In the sample exposed to wet supercritical CO_2, the presence of H_2S had no significant impact on carbonate formation. Exposure to a supercritical CO_2 phase in equilibrium with concentrated H_2SO_4, on the other hand, did result in a considerable difference in precipitated carbonate phases, with aragonite as the main carbonate phase, and calcite also more prevalent, while vaterite was suppressed. This also resulted in a somewhat higher overall carbonate content (41% vs. 36% or 34% for clean CO_2 or CO_2 with H_2S, respectively), indicating that the presence of H_2SO_4 and/or the reduced water content resulted in increased carbonate stability, and that the change in carbonate phases resulted from a promotion of aragonite and calcite formation more than a reduction of vaterite precipitation.

While 2 did report elevated S/Si-ratios in the inner parts of samples exposed to CO_2 with H_2S, and a minor elevation in S/Si-rations in the inner parts of samples exposed to CO_2 with H_2SO_4, only minor quantities of S-based phases were identified through XRD. These phases are Fe-sulphides (pyrite and pyrrhotites) and gypsum for both exposure to CO_2 with H_2S (CO_2-saturated water as well as wet supercritical CO_2) and to CO_2 with H_2SO_4.

Within the outer zones of samples, the impacts of H_2S and H_2SO_4 were more complicated. Focusing first on exposure to CO_2-saturated water, and comparing the compositions of the outer rims, we observe significant reductions in Ca-carbonate contents for both samples. However, in the sample exposed with H_2S, this reduction was considerably stronger, resulting in a lower overall Ca-carbonate content (19% vs. 22% for clean CO_2). Furthermore, while in both samples, calcite was the main Ca-carbonate and vaterite had been almost fully dissolved, the sample exposed to water saturated with clean CO_2 had a higher aragonite content (7% vs. 3%). These results support observations in 2, that the presence of H_2S during exposure to CO_2-saturated water resulted in lower carbonate contents and a greater degree of degradation in the outer rim. Exposure with H_2S also lead to the precipitation of significant amounts of Fe-sulphides (~2%) and gypsum (~2–3%). The presence of Fe-sulphides was also noted by 2, who reported the presence of submicron particles consisting of Fe and S, with approximately 1.5–2 S per Fe, throughout the samples exposed to CO_2 with H_2S. When comparing the top disc samples, a higher overall carbonate content (30%) was detected in the sample exposed to CO_2-saturated water with H_2S, compared to the sample exposed to clean CO_2 (25%), which can be ascribed to higher calcite (15% vs. 12%) and vaterite (7% vs. 4%) contents. This corresponds well to the higher vaterite and overall Ca-carbonate contents measured in the inner part of the H_2S-exposed sample, suggesting that here, the presence of H_2S mostly promoted initial Ca-carbonate precipitation but did not affect subsequent carbonate dissolution-reprecipitation. As in the inner part and outer rim, Fe-sulphides and gypsum were also detected in both the top and the bottom part of the sample exposed to CO_2-saturated water with H_2S, but their concentrations were too low for a quantitative comparisons.

As with clean CO_2, the precipitates that formed on the top surface of the sample exposed to CO_2-saturated water with H_2S consisted mostly of aragonite, which can be ascribed again to the Mg/Ca molar ratio of 1.9 measured in the aqueous exposure fluid at the end of the exposure[2]. However, the precipitates formed during exposure in the presence of H_2S show higher calcite peaks, indicating some calcite also formed here.

In the samples exposed directly to the CO_2-phase, comparing the outer rims, the presence of H_2S most notably led to a higher overall carbonate content (47% vs. 40%) driven by higher vaterite and calcite contents. However, a significantly higher aragonite content was measured in the sample exposed to clean CO_2 (9% vs. 2%). The higher Ca-carbonate content in the presence of H_2S measured here disagrees with the inference of 2, of somewhat lower carbonate contents in the outer rim of the sample exposed to wet supercritical CO_2 with H_2S, that was based on density contrasts in CT-scans and SEM micrographs. In addition, in the top disc sample the presence of H_2S resulted in the precipitation of a significant quantity of gypsum (5%), as well as minor Fe-sulphides. The presence of such a significant quantity of gypsum requires oxidation of the H_2S, which most likely took place through interactions with oxidized cations within the cement samples, such as Fe^{3+}. This observation therefore highlights the need for an improved understanding of the potential fate of impurities such as H_2S when injected into a geological reservoir during CO_2-injection and storage, and the potential reactions between such impurities and not only major, but also trace minerals within the GCS reservoir. Furthermore, the precipitation of gypsum also indicates the presence of SO_4^{2-} in the pore fluid. While this has been established to stabilise vaterite (cf. 15,18), no such effect was apparent here. Note that significant siderite, as might form when Fe^{2+} reacts with CO_3^{2-}, was not detected in this sample.

Comparing the sample exposed to wet supercritical CO_2 with H_2S to that exposed to CO_2-saturated water with H_2S, within the inner parts overall carbonate contents are lower in the former. However, exposure to CO_2-saturated water with H_2S resulted in a very strong reduction in carbonate content between the inner part and outer rim, while exposure to wet supercritical CO_2 with H_2S resulted in a further increase in carbonate content between the inner part and outer rim. This very strong reduction in carbonate content observed for exposure to CO_2-saturated water with H_2S correlates well to the reported higher degree of leaching compared to clean CO_2 based on analyses of exposure fluid chemical compositions[2].

In the sample exposed to CO_2 with H_2SO_4, the overall carbonate content in the inner part is higher than observed for clean CO_2 or CO_2 with H_2S, driven mostly by a significantly higher aragonite content. Overall carbonate contents in the outer parts of the sample exposed to CO_2 with H_2SO_4 fall within the range observed for the other samples exposed to the wet supercritical CO_2 phase, but do comprise significantly higher aragonite contents, especially when compared to the sample exposed to CO_2 with H_2S. Furthermore, compared to the samples exposed to other CO_2-compositions, the vaterite content in the inner part is much lower for the sample exposed to CO_2 with H_2SO_4. This vaterite then increases significantly in the outer parts analysed, while for the samples exposed to clean CO_2 or CO_2 with H_2S, except for the outer rim of the sample exposed to CO_2 with H_2S, the vaterite content decreased. While the higher vaterite content in the outer part of this sample could be a result of the SO_4^{2-} [15,18], somewhat elevated S-contents (S/Si-ratios) were measured throughout this sample using EDS (see 2), meaning that the presence of sulphate should then also have resulted in a higher vaterite content in the inner part of the sample. Furthermore, as established above, SO_4^{2-} also formed within the samples during exposure to CO_2 with H_2S. Therefore, it is more likely that in the outer part of the sample exposed to CO_2 with H_2SO_4, the dissolution of vaterite and subsequent precipitation of calcite and aragonite were inhibited by the

(partial) desiccation effect discussed by 2. This would also explain why the overall Ca-carbonate content in the outer zone is somewhat higher than in the inner zone (rather than being reduced as observed for clean CO_2 or CO_2 with H_2S), and why Ca-carbonate contents in both zones are higher than observed in the other samples exposed to wet supercritical CO_2. In addition, the overall carbonate contents are comparable to, if somewhat higher than, those measured in the outer rims of samples exposed to CO_2 for only 7 days, though in those samples, vaterite was the main carbonate, while only minor aragonite (2–3%) was present. This observation suggests that the relatively high aragonite contents in both the outer zone and inner zones of the sample exposed to CO_2 with H_2SO_4 are the result of a positive impact on aragonite formation rather than a negative impact on vaterite (or calcite) precipitation and preservation. Finally, while it has been established that SO_4^{2-} can increase aragonite stability relative to calcite (e.g., 19,20), the reduction in pore water content due to the desiccation effect during the exposure to CO_2 with H_2SO_4 potentially imposed a stronger control over Ca-carbonate polymorph selection. This is further supported by experimental research by 21, who reported the formation of aragonite during the exposure of crushed hydrated cement to CO_2 with H_2S under dry conditions.

Fate of S-compounds in CO_2-exposed cement

The concentrations of S-impurities in the exposure fluids were low. For exposure to CO_2 with H_2S, 1.6 mol% H_2S in the CO_2-phase resulted in 0.087 mol% H_2S in the H_2O-phase at initial equilibrium, while even lower concentrations were measured on retrieved fluid samples (see 2). During exposure to CO_2 with H_2SO_4, the maximum concentration of H_2SO_4 in CO_2 was 0.091×10^{-3} mol%. Regardless, the EDS-mapping reported in 2 showed elevated S-contents, expressed as S/Si-ratios, in all samples exposed to CO_2 with S-impurities, indicating that S-bearing minerals must have been present in these samples. One target of the present study was to identify these minerals, in order to better understand the fate of S-impurities in CO_2 when this CO_2 penetrates and reacts with a typical PC-based wellbore cement.

Significant concentrations of gypsum were detected in the top and bottom discs (5% and 1–2%, respectively) of the sample exposed to wet supercritical CO_2 with H_2S, as well as in the outer rim of the sample exposed to CO_2-saturated water with H_2S (2–3%). Otherwise, only negligible concentrations of gypsum (or anhydrite) were detected in any other samples. In the SEM study presented in 2, the presence of very small (submicron) particles composed of Fe and S (with about 1.5–2 S per Fe) was reported, indicating the potential formation of pyrite and/or pyrrhotites. In the XRD analyses presented here, Fe-sulphide concentrations (obtained by summing pyrite and pyrrhotite signals) were typically negligible to low (~1% or lower) in most samples. However, a concentration of almost 2% Fe-sulphides was measured in the outer rim of the sample exposed to CO_2-saturated water with H_2S. A similar apparent discrepancy between SEM/EDS and XRD was also reported by 22. Using SEM with EDS, they observed small (<5 μm) Fe-sulphide particles in Class H PC that had been exposed to CO_2 with 21 mol% H_2S at 50 °C. However, they did not detect significant quantities of Fe-sulphides in XRD, which they ascribed to Fe-sulphide particle sizes and crystallinities (see also 23).

The presence of Fe-sulphides is not surprising, and can be explained through direct interactions between the incoming H_2S, and Fe-bearing phases such as Fe-(hydr)oxides and brownmillerite in the exposed cement. However, the relatively high gypsum contents observed in the end discs of the sample exposed to wet supercritical CO_2 with H_2S and the outer rim of the sample exposed to CO_2-saturated water with H_2S are more interesting, as the formation of gypsum requires the oxidation of introduced sulphide within the cement microstructure, through the reduction of oxidized phases there. Such reduction, for example of Fe^{3+}, was already hypothesised in 2 based on the relatively dark, bluish colouration of the H_2S-exposed samples, and was also proposed by 22,24 who reported the precipitation of sulphate-bearing ettringite in samples of, respectively, Class H PC and pozzolan-amended PC, exposed to CO_2 with 21 mol% H_2S at 50 °C. Indeed, the high gypsum contents measured here correlate to very strong reductions in brownmillerite content (to well below 1%). Furthermore, while 22,24 reported the presence of ettringite, in the samples discussed here, gypsum formed instead, as ettringite does not form at temperatures above ~70 °C (during cement curing – cf. 25). Furthermore, the formation of (metastable) gypsum instead of (stable) anhydrite can be explained by the fact that at our exposure temperatures, anhydrite precipitation is kinetically inhibited (cf. 26,27). Note that the precipitation of gypsum has been reported for cement samples exposed to H_2S (without CO_2) at even higher temperatures (cf. 28 and references therein). The absence of gypsum in the inner part of our samples, while 22 reported ettringite mostly in the inner parts of their samples, indicates that in our experiments, gypsum formation may have been a secondary reaction with Ca^{2+} provided by the dissolution of the initially precipitated vaterite. The absence of significant gypsum or anhydrite in the sample exposed to supercritical CO_2 with H_2SO_4 can be explained by the low overall S-concentrations in the CO_2-phase, and therefore low quantities of SO_4^{2-} penetrating the exposed samples, but can also be related to the desiccation effect inhibiting further reaction after initial carbonate precipitation

Implications

The XRD analyses presented here, on cement samples exposed to wet supercritical CO_2 and CO_2-saturated water, using clean CO_2, CO_2 with H_2S and CO_2 with H_2SO_4 show that initial Ca-carbonate precipitation was, typically, dominated by metastable vaterite. During ongoing exposure, this vaterite then dissolved and partially reprecipitated as stable calcite or aragonite, while in samples exposed to CO_2-saturated water, a portion of the dissolved Ca^{2+} was removed from the sample by leaching into the aqueous exposure fluid. The initial precipitation of metastable vaterite, and the subsequent degree to which this is transformed into more stable calcite or aragonite may have implications for the long-term integrity of exposed wellbore cements, especially when they become significantly exposed to aqueous fluids, and therefore leaching.

The presented analyses further show, that, in addition to affecting the relative stability of calcite, vaterite, and aragonite,

even low concentrations of impurities (though, in the case of H_2S here, still well above concentrations that would be expected during GCS of captured CO_2) can have significant impacts on the resulting mineral assemblages. This is demonstrated most clearly in the top disc of the sample exposed to wet supercritical CO_2 with H_2S, where a low concentration of H_2S (~1.6 mol%) strongly reacted with brownmillerite (of which there was ~5% in the hydrated cement starting material), leading to the near-complete dissolution of the brownmillerite, and the precipitation of a relatively large quantity of gypsum (~5%). Similarly, in the outer rim of the sample exposed to CO_2-saturated water with H_2S, brownmillerite was almost completely removed, while 2–3% gypsum was formed, as well as significant Fe-sulphides, and siderite.

Pore clogging due to Ca-carbonate precipitation has long been established as an effective mechanism for limiting diffusion, and therefore the inward progress of carbonation (e.g., 29–35). Considering gypsum's large molar volume (74 cm^3/mol vs. 37 cm^3/mol for calcite), gypsum precipitation presents a considerably enhanced pore clogging potential, implying more effective inhibition of diffusion deeper into a cement-based well barrier. However, the long-term efficiency of pore clogging by gypsum will also be dependent on the stability of gypsum, and the potential transformation of gypsum to anhydrite or Ca-carbonate with associated decreases in molar volume.

These results thus demonstrate that even at low concentrations, impurities in CO_2 can have relatively large impacts on both short- and long-term integrity of cement-based seals in wells through reactions with both main and minor mineral phases that affect the resulting mineral compositions. Furthermore, these impacts may be significantly different for exposure to CO_2-saturated water compared to (wet) supercritical CO_2. Therefore, models forecasting the long-term behaviour and integrity of cement-based seals must incorporate a thorough understanding of any relevant impurities, which needs to be based on experimental research. Further experimental research is thus required, exposing cement samples (as well as other relevant materials) to different impure CO_2-compositions at relevant conditions (i.e., in-situ pressures and temperatures; (wet) supercritical CO_2 vs. CO_2-saturated water or brine; and impurity compositions and contents), and then employing a wide range of analytical techniques, on different scales, to identify and comprehend microstructural, chemical and mineralogical changes in the exposed samples. Both these experiments and the resulting models need to take into account the potential initial formation of metastable phases, such as vaterite and gypsum, as well as any subsequent transformation (through dissolution-reprecipitation or other mechanisms) into more stable phases.

In addition, the impact of impurities may be more pronounced along potential leakage pathways such as the cement-steeI and cement-caprock interfaces or cracks through the cement (as also argued in 2). Here, additional reactions may take place, for example with the steel wellbore, while a flow of impure CO_2 along a leaky interface or crack can expose the sidewalls to much greater quantities of reactive impurities. Therefore, the role of these interfaces and any interplay with (reactive) impurities needs to be assessed experimentally as well. Quite different mineral assemblages were indeed observed in some of the end discs analysed here, compared to the outer rims of the same samples (cf. the top discs of samples exposed to clean wet supercritical CO_2 and wet supercritical CO_2 with H_2S), showing that different chemical environments can indeed develop and exist at relatively small scales (i.e., within our cylinders with total length 30 mm), even at nominally static exposure conditions, and that these different environments may result in quite different mineral assemblages. These observations reaffirm the importance of accurately simulating, both in experiments and numerical models, the expected exposure environment(s) to obtain representative results, and avoid (experimental) artefacts. Finally, the results presented that are complementary to the work presented previously 1,2 also demonstrate the importance of using a wide range of analysis to thoroughly assess microstructural and chemical changes as well as changes in mineral compositions to fully understand how complex materials such as cements are affected by exposure to CO_2 with and without (reactive) impurities. Further work is also needed to address the impact of other (reactive) impurities and combinations of impurities that have not yet been tested experimentally.

Conclusions

XRD analyses were performed on samples of cement (Class G PC with 35% by weight of cement silica flour – Cementegrity S1) that had been exposed to (wet) supercritical CO_2 and CO_2-saturated water, using clean CO_2, CO_2 with 1.6 mol% H_2S, and CO_2 in equilibrium with concentrated H_2SO_4. These are the main findings:

- Ca-carbonates initially precipitated predominantly as metastable vaterite. During ongoing exposure, this vaterite was then partly replaced by more stable calcite and aragonite, most likely through a dissolution-precipitation process. In samples exposed to CO_2-saturated water, this transformation was associated with a reduction in overall crystalline carbonate content, while in samples exposed to (wet) supercritical CO_2, carbonate contents further increased.
- In the samples exposed to CO_2-saturated water, the presence of H_2S mostly promoted initial precipitation of Ca-carbonates, especially vaterite. During continued exposure, however, a stronger reduction in Ca-carbonate was observed with H_2S, leading to a lower overall carbonate content. Furthermore, (minor) Fe-sulphides and gypsum were detected after exposure with H_2S, especially in the outer rim of the sample.
- In the samples exposed to wet supercritical CO_2, the presence of H_2S did not significantly impact initial Ca-carbonate precipitation. However, during ongoing exposure, Ca-carbonate contents increased more significantly than without H_2S, with both calcite and vaterite contents increasing. Furthermore, in the top part of the exposed sample, significant gypsum was detected, which was associated with the almost complete disappearance of brownmillerite.

- In the samples exposed to supercritical CO_2 with H_2SO_4, within the inner part of the sample, aragonite was the main Ca-carbonate, while calcite was also promoted and vaterite was suppressed. This resulted in higher overall (crystalline) Ca-carbonate contents. In the outer parts, vaterite was the main carbonate, while aragonite contents were relatively high. While SO_4^{2-} is known to affect Ca-carbonate polymorph stability, the desiccation effect caused by the presence of concentrated H_2SO_4 within the reaction vessel likely imparted a stronger impact on mineral changes here. Only very minor Fe-sulphides and gypsum and/or anhydrite were detected using XRD.

- Significant gypsum was detected in outer parts of samples exposed to CO_2 with H_2S, and associated with a strong local decrease in brownmillerite content. These observations indicate that Ca^{2+} was most likely provided by the dissolution of initially precipitated, metastable vaterite, while the oxidation of S^{2-} to form SO_4^{2-} proceeded through the reduction of Fe^{3+} (from brownmillerite) to Fe^{2+}.

- This oxidation of sulphide to sulphate presents an important mechanism controlling the fate of the H_2S-impurity upon entering a cement-based sealant. Similar reactions with reservoir minerals should also be expected, with potentially relatively large impacts in the near-wellbore area.

- While the impacts of the impurities tested here were, overall, relatively minor, the precipitation of a significant quantity of gypsum upon exposure to CO_2 with H_2S was a significant change, demonstrating the need for a thorough understanding of potential impurity-mineral interactions, in order to properly forecast long-term wellbore seal integrity during the injection and storage of CO_2 with impurities.

- The impact of even low concentrations of impurities may be greatly enhanced along leakage pathways (i.e., cracks or leaky interfaces) in the well system, where a flow of CO_2 may continuously provide a supply of impurities.

Ethics and consent

Ethical approval and consent were not required.

Data availability

Raw data from all XRD analyses discussed in this article is included in the underlying data file, which has been uploaded to Zenodo (https://doi.org/10.5281/zenodo.18301363)[5].

Data are available under the terms of the Creative Commons Attribution 4.0 International

Acknowledgement

David Wragg's instruction and support in the performance of the X-ray powder diffraction analyses and subsequent Rietveld refinements and quantifications is gratefully acknowledged.

References

1. Van Noort R, Svenningsen G, Li K, *et al.*: **Exposure of five cementitious sealant materials to wet supercritical CO_2 and CO_2-saturated water under simulated downhole conditions.** *Int J Greenh Gas Con.* 2025; **144**: 104380.
Publisher Full Text

2. Van Noort R, Svenningsen G, Li K: **Experimental study on the impact of H_2S and H_2SO_4 in CO_2 on five different sealant compositions under conditions relevant for geological CO_2-storage.** *Geoenergy Sci Eng.* 2025; **253**: 214005.
Publisher Full Text

3. Van Noort R, Yarushina Y: **Comparison of forced-flow and batch exposures of a representative wellbore cement to CO_2, and implications for extrapolation from laboratory to field.** 13th Trondheim Carbon Capture and Storage Conference (TCCS), 16/06-19/06, Trondheim (N). 2025.
Reference Source

4. Coelho AA: ***TOPAS* and *TOPAS-Academic*: an optimization program integrating computer algebra and crystallographic objects written in C++.** *J Appl Cryst.* 2018; **51**(1): 210–218.
Publisher Full Text

5. Van Noort R: **Raw XRD data and spectra for the paper "XRD analyses on silica-amended Class G cement samples exposed to clean and impure CO_2 in the presence of water".** *Zenodo.* 2026.
http://www.doi.org/10.5281/zenodo.18301363

6. Ogino T, Suzuki T, Sawada K: **The formation and transformation mechanism of calcium carbonate in water.** *Geochim Cosmochim Acta.* 1987; **51**(10): 2757–2767.
Publisher Full Text

7. Kralj D, Brečević L, Kontrec J: **Vaterite growth and dissolution in aqueous solution III. Kinetics of transformation.** *J Cryst Growth.* 1997; **177**(3–4): 248–257.
Publisher Full Text

8. Han YS, Hadiko G, Fuji M, *et al.*: **Crystallization and transformation of vaterite at controlled pH.** *J Cryst Growth.* 2006; **289**(1): 269–274.
Publisher Full Text

9. Kitamura M: **Strategy for control of crystallization of polymorphs.** *CrystEngComm.* 2009; **11**(6): 949–964.
Publisher Full Text

10. Prah J, Maček J, Dražič G: **Precipitation of calcium carbonate from a calcium acetate and ammonium carbamate batch system.** *J Cryst Growth.* 2011; **324**(1): 229–234.
Publisher Full Text

11. Udrea I, Capa C, Olaru EA, *et al.*: **Vaterite synthesis via gas-liquid route under controlled pH conditions.** *Ind Eng Chem Res.* 2012; **51**(24): 8185–8193.
Publisher Full Text

12. Konopacka-Łyskawa D, Kościelska B, Łapiński M: **Precipitation of spherical vaterite particles via carbonation route in the bubble column and the gas-lift reactor.** *JOM.* 2019; **71**: 1041–1048.
Publisher Full Text

13. Chen J, Xiang L: **Controllable synthesis of calcium carbonate polymorphs at different temperatures.** *Powder Technol.* 2009; **189**(1): 64–69.
Publisher Full Text

14. Hanifa M, Sharma U, Thapliyal PC, *et al.*: **Effects of temperature, pH and calcium-to-carbonate ratio on the calcium carbonate polymorphs.** *Discov Civ Eng.* 2025; **2**: 147.
Publisher Full Text

15. Zhao D, Williams JM, Hou P, *et al.*: **Stabilizing mechanisms of metastable vaterite in cement systems.** *Cem Concr Res.* 2024; **178**: 107441.
Publisher Full Text

16. Niedermayr A, Köhler SJ, Dietzel M: **Impacts of aqueous carbonate**

accumulation rate, magnesium and polyaspartic acid on calcium carbonate formation (6-40°C). *Chem Geol.* 2013; **340**: 105–120.
Publisher Full Text

17. Park WK, Ko SJ, Lee SW, *et al.*: **Effects of magnesium chloride and organic additives on the synthesis of aragonite precipitated calcium carbonate.** *J Cryst Growth.* 2008; **310**(10): 2593–2601.
Publisher Full Text

18. Fernández-Díaz L, Fernández-González Á, Prieto M: **The role of sulfate groups in controlling $CaCO_3$ polymorphism.** *Geochim Cosmochim Acta.* 2010; **74**(21): 6064–6076.
Publisher Full Text

19. Bischoff JL, Fyfe WS: **Catalysis, inhibition, and the calcite-aragonite problem; [Part] 1, The aragonite-calcite transformation.** *Am J Sci.* 1968; **266**(2): 65–79.
Publisher Full Text

20. Forjanes P, Astilleros JM, Fernández-Díaz L: **The role of sulfate in the hydrothermal replacement of aragonite single crystals by calcite.** *Earth Planet Sci Lett.* 2024; **639**: 118771.
Publisher Full Text

21. Jacquemet N, Pironon J, Saint-Marc J: **Mineralogical changes of a well cement in various H_2S-CO_2(-Brine) fluids at high pressure and temperature.** *Environ Sci Technol.* 2008; **42**(1): 282–288.
PubMed Abstract | Publisher Full Text

22. Kutchko BG, Strazisar BR, Hawthorne SB, *et al.*: **H_2S-CO_2 reaction with hydrated Class H well cement: acid-gas injection and CO_2 co-sequestration.** *Int J Greenh Gas Con.* 2011; **5**(4): 880–888.
Publisher Full Text

23. Michel FM, Antao SM, Chupas PJ, *et al.*: **Short- to medium-range atomic order and crystallite size of the initial FeS precipitate from pair distribution function analysis.** *Chem Mater.* 2005; **17**(25): 6246–6255.
Publisher Full Text

24. Zhang L, Dzombak DA, Nakles DV, *et al.*: **Characterization of pozzolan-amended wellbore cement exposed to CO_2 and H_2S gas mixtures under geologic carbon storage conditions.** *Int J Greenh Gas Con.* 2013; **19**: 358–368.
Publisher Full Text

25. Taylor HFW, Famy C, Scrivener KL: **Delayed ettringite formation.** *Cem Concr Res.* 2001; **31**(5): 683–693.
Publisher Full Text

26. Freyer D, Voigt W: **Crystallization and phase stability of $CaSO_4$ and $CaSO_4$ - Based salts.** *Monatsh für Chem.* 2003; **134**: 693–719.
Publisher Full Text

27. Azimi G, Papangelakis VG: **Mechanism and kinetics of gypsum-anhydrite transformation in aqueous electrolyte solutions.** *Hydrometallurgy.* 2011; **108**(1–2): 122–129.
Publisher Full Text

28. Yin Y, Zhang L, Mei K, *et al.*: **Experimental investigation on H_2S-induced oilwell cement degradation under high-temperature conditions for geothermal applications.** *Geothermics.* 2024; **121**: 103023.
Publisher Full Text

29. Kutchko BG, Strazisar BR, Dzombak DA, *et al.*: **Degradation of well cement by CO_2 under geologic sequestration conditions.** *Environ Sci Technol.* 2007; **41**(13): 4787–4792.
PubMed Abstract | Publisher Full Text

30. Kutchko BG, Strazisar BR, Lowry GV, *et al.*: **Rate of CO_2 attack on hydrated class H well cement under geologic sequestration conditions.** *Environ Sci Technol.* 2008; **42**(16): 6237–6242.
PubMed Abstract | Publisher Full Text

31. Duguid A: **An estimate of the time to degrade the cement sheath in a well exposed to carbonated brine.** *Energy Procedia.* 2009; **1**(1): 3181–3188.
Publisher Full Text

32. Wigand M, Kaszuba JP, Carey JW, *et al.*: **Geochemical effects of CO_2 sequestration on fractured wellbore cement at the cement/caprock interface.** *Chem Geol.* 2009; **265**(1–2): 122–133.
Publisher Full Text

33. Jacquemet N, Pironon J, Lagneau V, *et al.*: **Armouring of well cement in H_2S-CO_2 saturated brine by calcite coating - Experiments and numerical modelling.** *Appl Geochem.* 2012; **27**(3): 782–795.
Publisher Full Text

34. Brunet JPL, Li L, Karpyn ZT, *et al.*: **Dynamic evolution of cement composition and transport properties under conditions relevant to geological carbon sequestration.** *Energy Fuels.* 2013; **27**(8): 4208–4220.
Publisher Full Text

35. Cheshire MC, Stack AG, Carey JW, *et al.*: **Wellbore cement porosity evolution in response to mineral alteration during CO_2 flooding.** *Environ Sci Technol.* 2016; **51**(1): 692–698.
PubMed Abstract | Publisher Full Text

Open Peer Review

Current Peer Review Status: ✔

Version 1

Reviewer Report 22 June 2026

https://doi.org/10.21956/openreseurope.24787.r72818

© **2026 Marsh A et al.** This is an open access peer review report distributed under the terms of the Creative Commons Attribution License, which permits unrestricted use, distribution, and reproduction in any medium, provided the original work is properly cited.

✔ **Alastair Marsh**
Ecole Polytechnique Federale de Lausanne Laboratory, Lausanne, Vaud, Switzerland
Sudharsan Rathna Kumar
LMC, Ecole Polytechnique Federale de Lausanne, Lausanne, Vaud, Switzerland

In this paper the author uses XRD analyses provide an analysis on the changes which occur when Class G Portland cement typically used in subsurface wells is exposed to CO2. They also show the role of other impurity phases like H2S, H2SO4 on the chemistry and phase assemblage. They present important implications of this research which would be important in CCS applications.

There are no critical flaws that need to be addressed. However, here are some points that the author could consider to further improve this manuscript:

1. The conversion between initial formation of vaterite to other polymorphs (calcite or aragonite) is particularly interesting. Please consider elucidating the role of amorphous calcium carbonate formation in this. While quantification might be difficult using XRD, the role of cross-conversion may be enhanced or abated by the formation of amorphous calcium carbonate.
2. The implications of the conversion might be rather problematic if there is a decrease in the integrity of the structure in question. This is also crucial since vaterite has the lowest density and thus the highest molar volume compared to calcite. It would be worthwhile to comment on the strength and stability of the well post exposure.
3. Another observation although SEM+EDS showed close similarities upon exposure wet, supercritical CO2 and CO2 saturated water, however leaching and degradation was observed in the case of wet, supercritical CO2. How much of this could be due to the sample preparation induced changes in the chemical analysis since different rims and locations were used? Please consider mentioning the role of preparation in observed chemical analysis.
4. Also, although it can be understood as saturated conditions meaning high RH close to 100%, it would be worthwhile to mention the RH values if measured. Especially the role of as a facilitator to the polymorph conversion should be mentioned.
5. An important phenomenon observed is the gypsum formation, which due to its larger

molar volume occupies more space, thus clogging pores. In the sample with wet sc CO2 with H2S as the impurity the highest amount of gypsum was observed. The oxidation of S2- to SO42- and Ca ions provided by the dissolution of vaterite should have led to lower vaterite content than calcite for the top disc. But this is not observed here. Is there another explanation for this particular case? Please consider clarifying.

6. There is a substantial degree of repetition for some statements, between the Results, Discussion and Implications, Implications and Conclusions. So, whilst the level of detail around the observations is very good, the article is much longer than expected (considering the quantity of results presented). If the repetition can be reduced, this will make a better experience for readers.

Is the work clearly and accurately presented and does it cite the current literature?
Yes

Is the study design appropriate and does the work have academic merit?
Yes

Are sufficient details of methods and analysis provided to allow replication by others?
Yes

If applicable, is the statistical analysis and its interpretation appropriate?
Not applicable

Are all the source data underlying the results available to ensure full reproducibility?
Yes

Are the conclusions drawn adequately supported by the results?
Yes

Competing Interests: No competing interests were disclosed.

Reviewer Expertise: The chemistry of Portland-based cements, and carbonation mechanisms.

We confirm that we have read this submission and believe that we have an appropriate level of expertise to confirm that it is of an acceptable scientific standard.